Supplementary Information

For

PPM1D Mutations Silence NAPRT Gene Expression and Confer Exquisite NAMPT Inhibitor Sensitivity in Glioma

Authors: Nathan R. Fons[1,2], Ranjini K. Sundaram[2], Gregory A. Breuer[1,2], Sen Peng[3], Ryan L. McLean[2], Aravind N. Kalathil[2], Mark Schmidt[4], Diana M. Carvalho[5], Alan Mackay[5], Chris Jones[5], Ángel M. Carcaboso[6], Javad Nazarian[7], Michael E. Berens[3*], Charles Brenner[4*], Ranjit S. Bindra[1,2*]

Supplementary Figure 1.

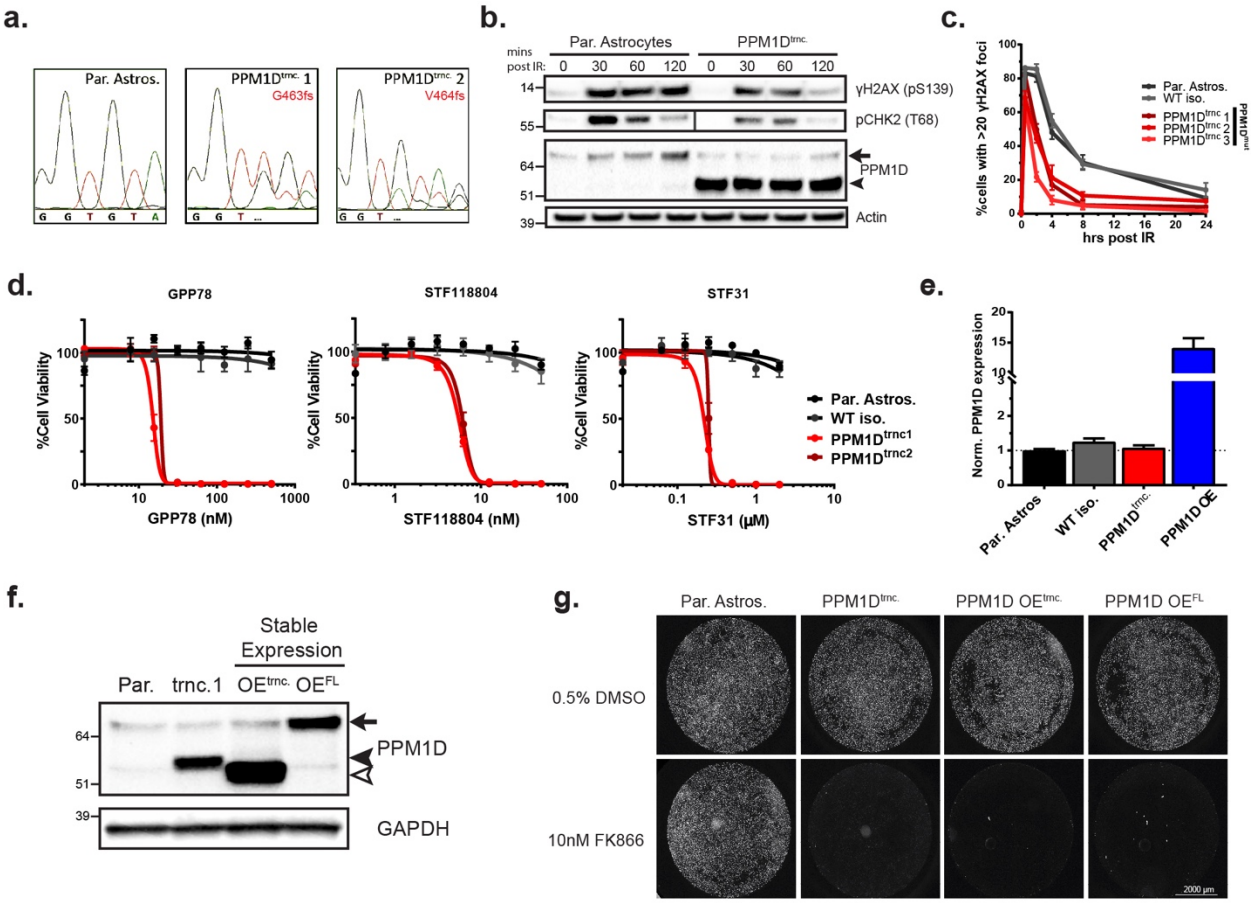

Supplementary Fig. 1. *PPM1D* mutant astrocytes are sensitive to NAMPT inhibitors. (**a**) Sequencing chromatograms within a region of *PPM1D* exon 6 from parental and PPM1D$^{trnc.}$ cell lines. (**b**) Immunoblot of parental and PPM1D$^{trnc.}$ cell lines in response to radiation. Full length (full arrow) and CRISPR-modified (arrowhead) sizes of PPM1D displayed. (**c**) Quantification of γH2AX foci post radiation (IR) (n=4 independent samples). (**d**) Viability assessments of cell lines after 72hr treatment with three different NAMPT inhibitors (GPP78, STF118804, and STF31) (n =3 independent samples). (**e**) Quantification of *PPM1D* transcript levels in astrocyte cell lines (n =4 independent samples). (**f**) Immunoblot of astrocytes with stable expression of wild type (OE^{FL}) or mutant (OE$^{trnc.}$) PPM1D. Full length (full arrow), CRISPR-edited (black arrowhead), and ectopically-expressed mutant protein (white arrowhead) sizes of PPM1D are displayed. (**g**) Representative wells of H33342-stained nuclei from parental and mutant astrocytes, 72hrs post DMSO or FK866 treatment. Error bars represent standard deviation of the mean.

Supplementary Figure 2.

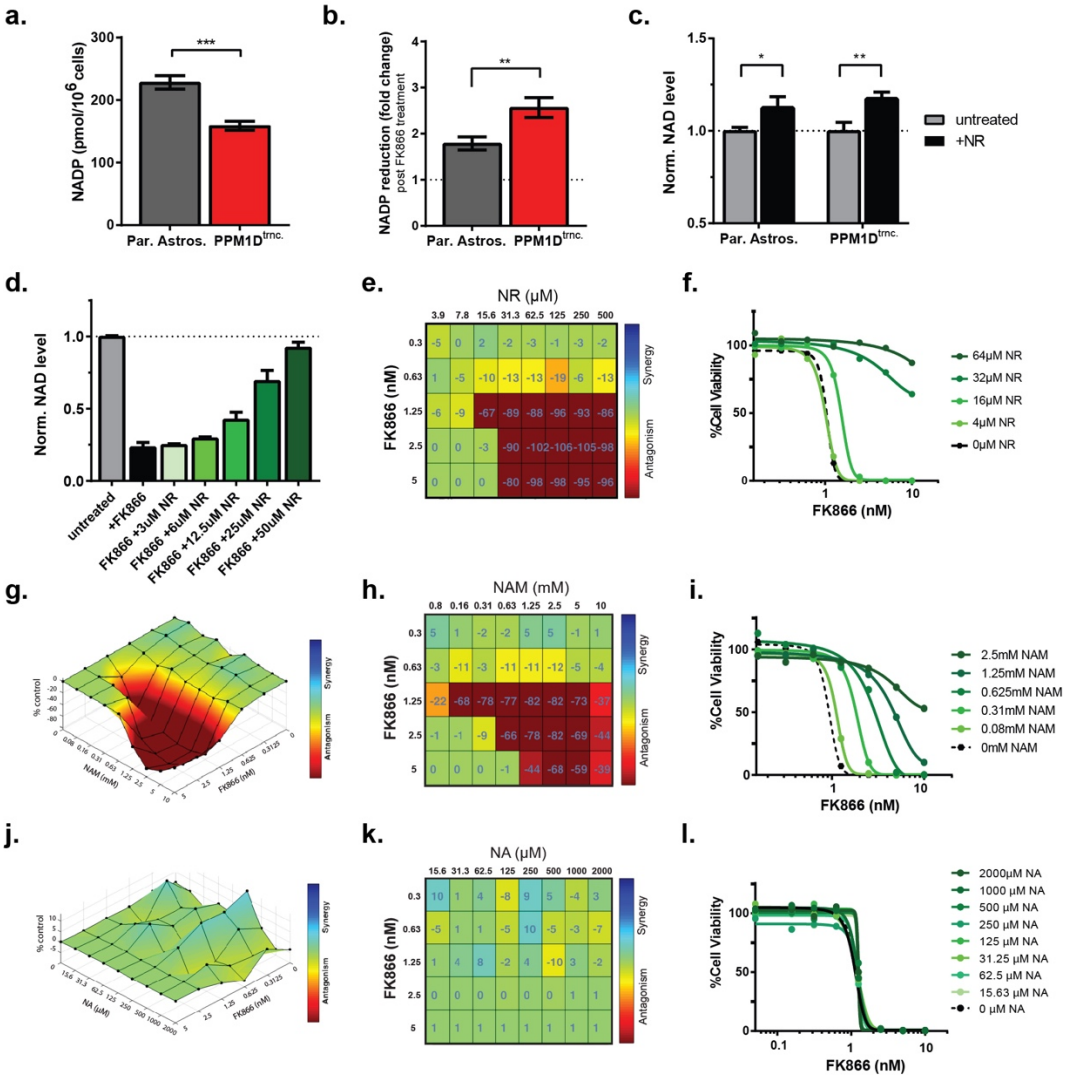

Supplementary Fig. 2. NAD metabolome depression in PPM1D$^{trnc.}$ astrocytes results in NAMPT inhibitor sensitivity. (**a**) NADP quantification in parental and PPM1D$^{trnc.}$ astrocytes (n=3 independent samples, *** p<0.001 by Student's T test). (**b**) Relative fold change in NADP levels after treatment with 10nM FK866 for 24hrs (n=3 independent samples, ** p<0.01 by Student's T test). (**c**) NAD quantification after exogenous addition of 50μM nicotinamide riboside (NR) for 24 hrs (n=3 independent samples, * p<0.05, ** p<0.01 by Student's T test). (**d**) Normalized NAD levels in astrocytes after 24hr treatment with 10nM FK866 and indicated doses of NR (n=2 independent samples). (**e**) Bliss model matrix for the antagonistic effects of NR on FK866 treatment in PPM1D$^{trnc.}$ astrocytes. (**f**) Viability assessment of PPM1D$^{trnc.}$ astrocytes after 72hr concurrent FK866 and NR treatment. (**g, j**) Bliss 3D surface plots modelling the antagonistic effects of NAM (g) or NA (j) on FK866 treatment in PPM1D$^{trnc.}$ astrocytes. (**h, k**) Bliss model matrices for the antagonistic effects of NAM (h) or NA (k) on FK866 treatment in PPM1D$^{trnc.}$ (**i, l**) Viability assessment of PPM1D$^{trnc.}$ astrocytes after 72hr concurrent treatment of FK866 with NAM (i) or NA (l). Error bars represent standard deviation of the mean.

Supplementary Figure 3.

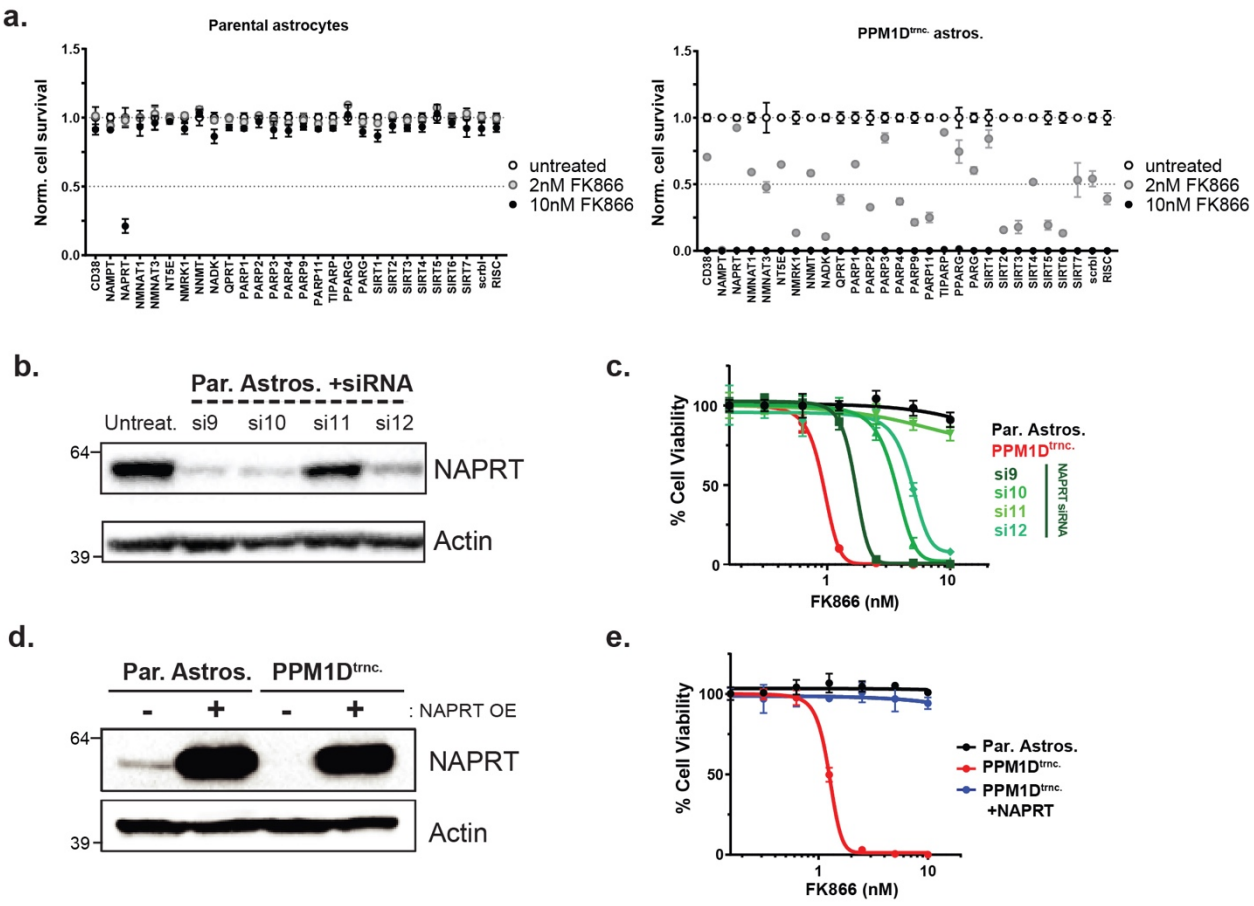

Supplementary Fig. 3. NAPRT deficiency drives sensitivity of *PPM1D* mutant astrocytes to NAMPT inhibitors. (**a**) Normalized viability of parental (*left*) and PPM1D$^{trnc.}$ (*right*) astrocytes to FK866 treatment after transfection with a panel of siRNAs targeting NAD biosynthesis-related enzymes (n=2 independent samples). (**b**) Immunoblot of NAPRT protein level after treatment with different NAPRT-targeted siRNAs. (**c**) Viability analysis of cell lines in b., treated with FK866 for 72hrs (n=4 independent samples). (**d**) Immunoblot of parental and PPM1D$^{trnc.}$ astrocytes +/- stable expression of NAPRT. (**e**) Viability assessment Par. Astros., PPM1D$^{trncs.}$, and a NAPRT-expressing PPM1D$^{trnc.}$ (PPM1D$^{trnc.}$+ NAPRT) cell line upon 72hr FK866 treatment (n=4 independent samples). Error bars represent standard deviation of the mean.

Supplementary Figure 4.

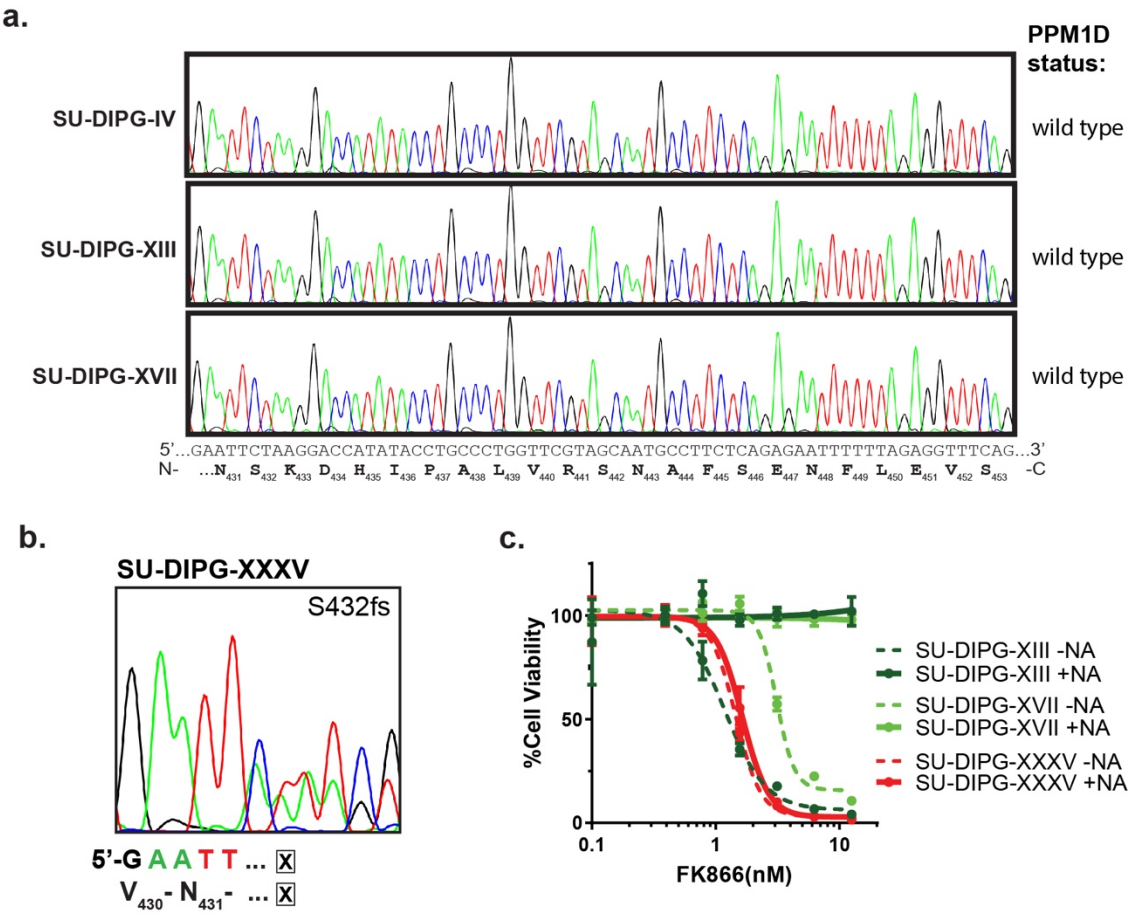

Supplementary Fig. 4. Patient-derived SU-DIPG-XXXV spheroid cell line possesses a truncating PPM1D mutation and is sensitive to NAMPT inhibitors. (**a**) Sequencing chromatograms within a region of *PPM1D* exon 6, from SU-DIPG-IV, XIII, and XVII spheroid cell lines. (**b**) Chromatogram of PPM1D-truncating mutation in SU-DIPG-XXXV. (**c**) Viability assessments of SU-DIPG spheroids to FK866 in nicotinic acid (NA) containing (+NA) or NA lacking (-NA) culture media (n=3 independent samples). Error bars represent standard deviation of the mean.

Supplementary Figure 5.

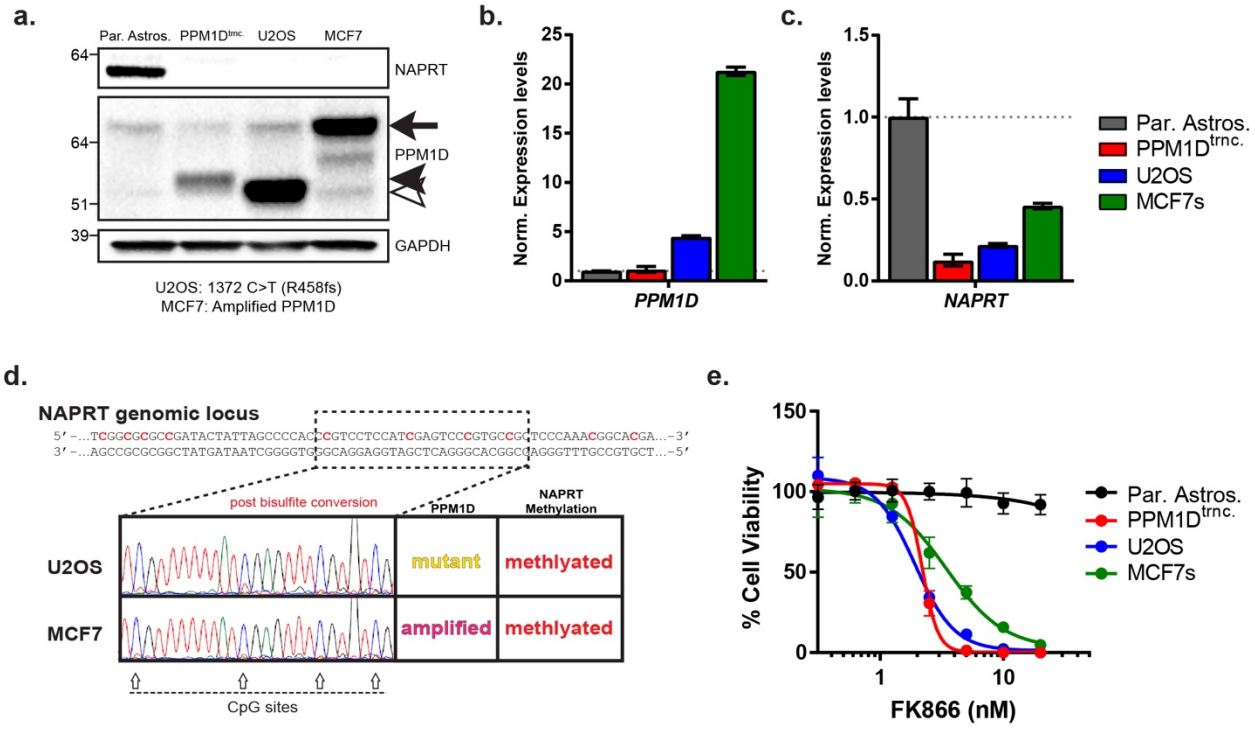

Supplementary Fig. 5. U2OS and MCF7 cell lines contain *PPM1D* alterations, silence *NAPRT* transcription, and are sensitive to NAMPT inhibitors. (**a**) Immunoblot of isogenic astrocytes, U2OS, and MCF7 cell lines. (**b, c**) Normalized mRNA expression of *PPM1D* (b) and *NAPRT* (c) in cell panel from a (n=4 independent samples). Error bars represent 95% Confidence Interval about the mean. (**d**) Sequencing chromatograms of the *NAPRT* promoter within U2OS and MCF7 cell lines after bisulfite conversion; arrows indicate potential CpG methylation sites. (**e**) Viability assessment of isogenic astrocytes, U2OS, and MCF7 cell lines after 96hr treatment with FK866 (n=3 independent samples). Error bars represent standard deviation of the mean.

Supplementary Figure 6.

a.

DIPG line	PPM1D	Histone 3 mutation	p53
HSJD-DIPG-007	P428fs	H3.3 (K27M)	WT
HSJD-DIPG-008	R429fs	H3.3 (K27M)	WT
HSJD-DIPG-14b	L484fs	H3.3 (K27M)	WT
SU-DIPG-IV	WT	H3.1 (K27M)	WT
SU-DIPG-XIII	WT	H3.3 (K27M)	WT
SU-DIPG-XVII	WT	H3.3 (K27M)	ND
SU-DIPG-XXXV	S432fs	H3.3 (K27M)	WT

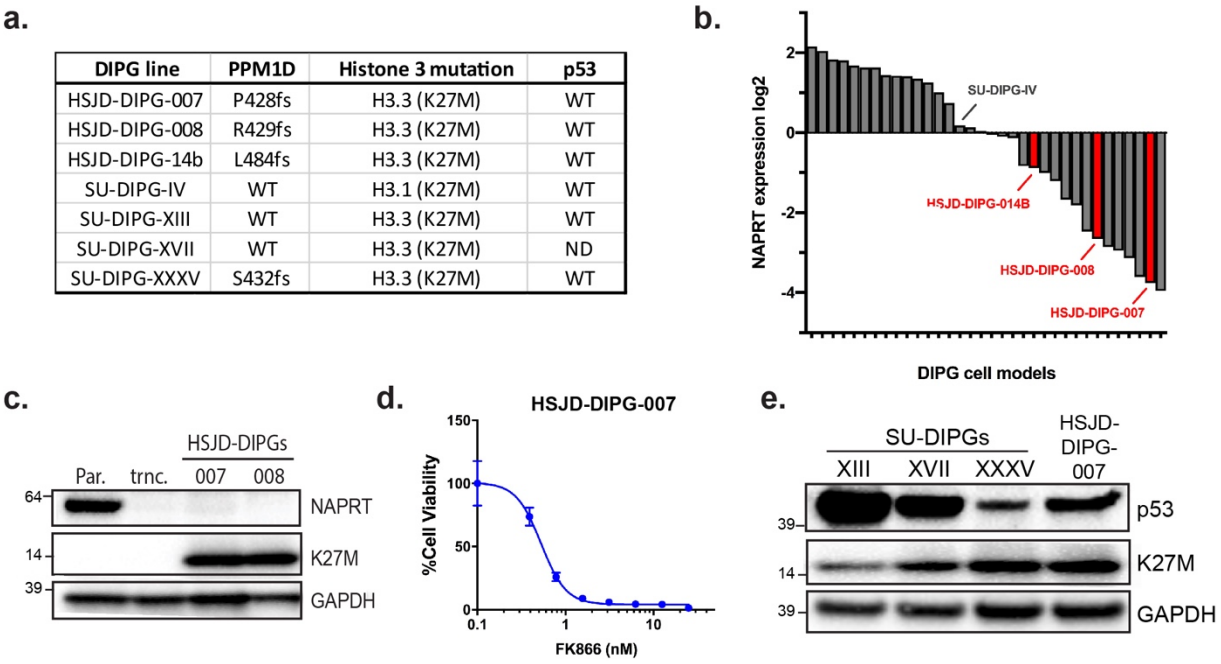

Supplementary Fig. 6. DIPG model cell lines with *PPM1D* mutations have reduced NAPRT expression and maintain p53 expression. (**a**) Table depicting mutational status of patient-derived DIPG cell lines in Fig 3e; ND indicates no data available. (**b**) *NAPRT* expression levels of model DIPG cell lines. (**c**) Immunoblot of select astrocyte and DIPG cell lines for NAPRT and H3K27M expression. (**d**) Viability of HSJD-DIPG-007 cell line after 120hr of treatment with FK866 (n=5 independent samples). Error bars represent standard deviation of the mean. (**e**) Immunoblot of DIPG cell line panel for p53 and H3K27M expression.

Supplementary Figure 7.

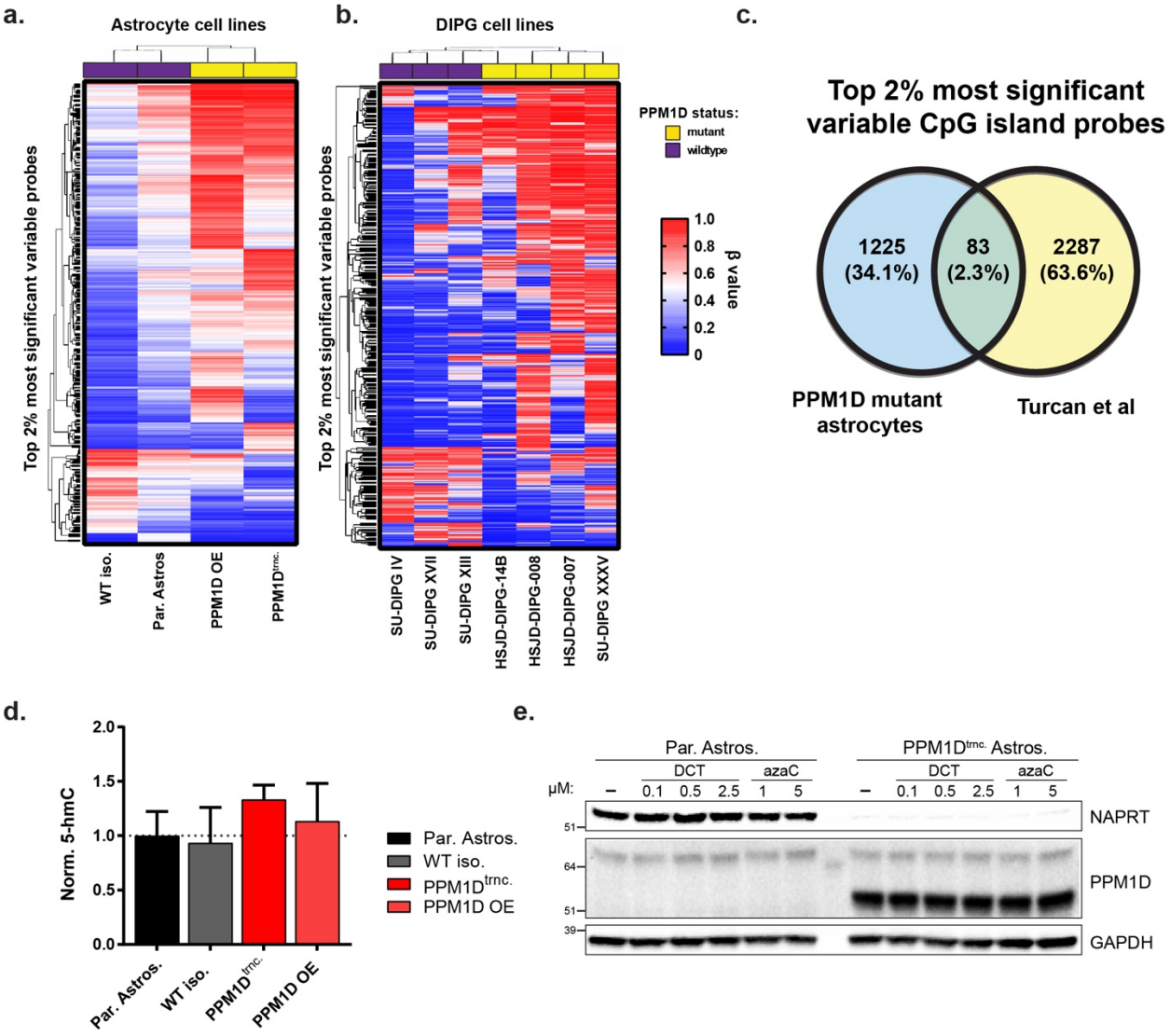

Supplementary Fig. 7. Mutant PPM1D-induced hypermethylation is distinct from G-CIMP found in *IDH1* mutant astrocytes. (**a, b**) Hierarchical clustering of the top 2% of significantly variable methylation probes in astrocyte (a) and DIPG (b) cell lines. (**c**) Comparison of top 2% significantly variable CpG island probe sets in *PPM1D* mutant- and *IDH1* mutant astrocytes (*30*). (**d**) Normalized levels of global 5-hydroxymethylcytosine in WT and *PPM1D* mutant astrocytes (n=4 independent samples). Error bars represent 95% Confidence Interval about the mean. (**e**) Immunoblot of parental and PPM1D$^{trnc.}$ astrocytes after treatment with varying doses of decitabine (DCT) or azacytidine (azaC) for 72hrs.

Supplementary Figure 8.

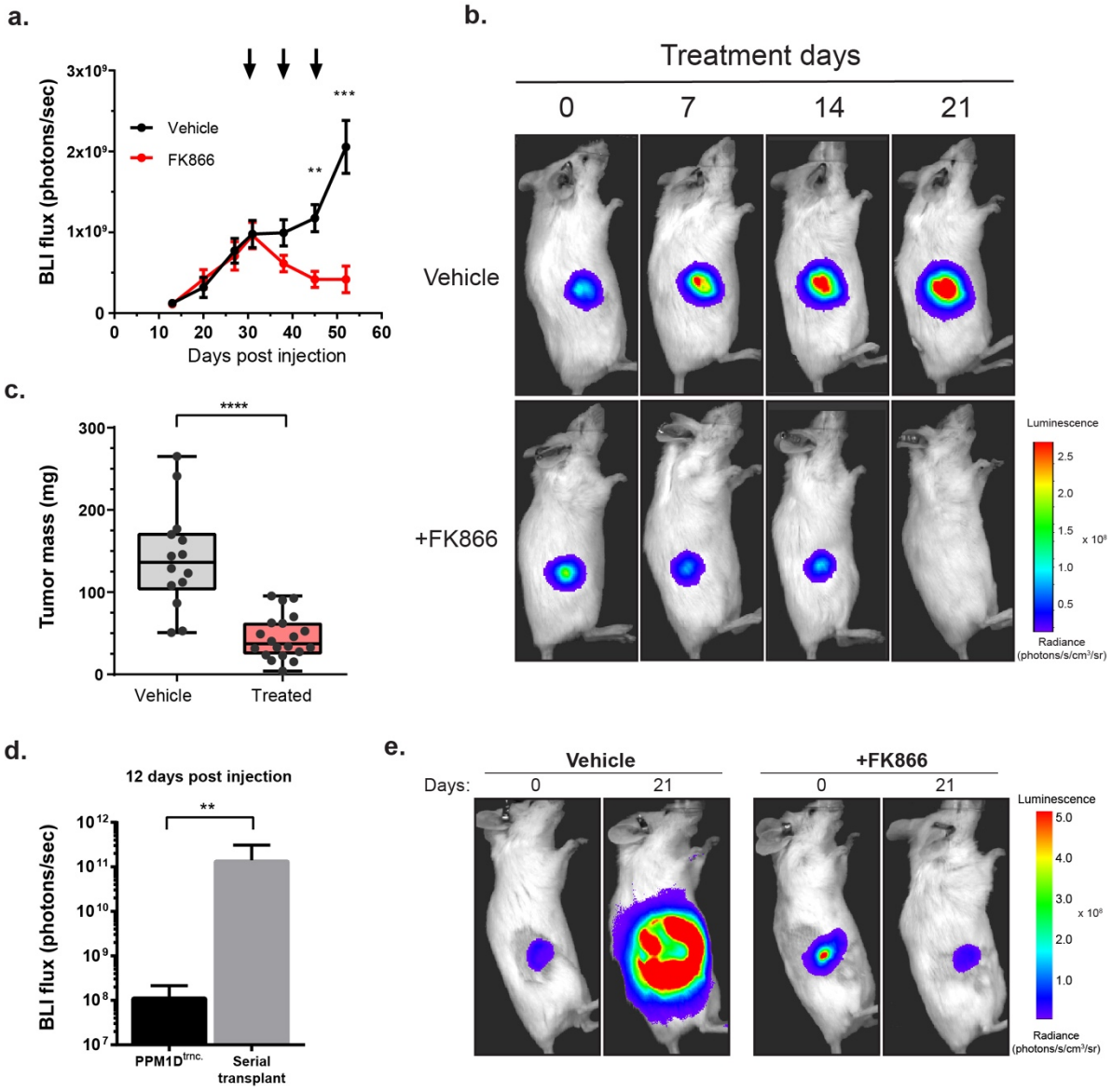

Supplementary Fig. 8. *In vivo* efficacy of NAMPT inhibitors in *PPM1D* mutant tumors. (**a**) PPM1D$^{trnc.}$ tumor burden as a measure of bioluminescence imaging (BLI) signal, in NOD *scid* gamma mice treated with vehicle or 20mg/kg FK866 BID for 3 four day cycles as indicated by arrows (n=10 independent animals, error bars represent SE, ** $p<0.01$, *** $p<0.001$ by Mann-Whitney U test). (**b**) Representative BLI images of vehicle and FK866-treated mice over course of treatment. (**c**) Tumor mass measurements, from extracted tumors in a., 2 months post injection (n=14 independent tumors, **** $p<0.0001$ by Student's T test). (**d**) Comparison of BLI signal intensity between PPM1D$^{trnc.}$ cell line xenografts and serially-transplanted *PPM1D* mutant xenografts, 12 days post injection (n=17 independent tumors, ** $p<0.01$ by Student's T test). Error bars represent standard deviation of the mean. (**e**) Representative BLI images of serially-transplanted *PPM1D* mutant xenografts before or after 3 weeks of indicated treatment.

Supplementary Figure 9.

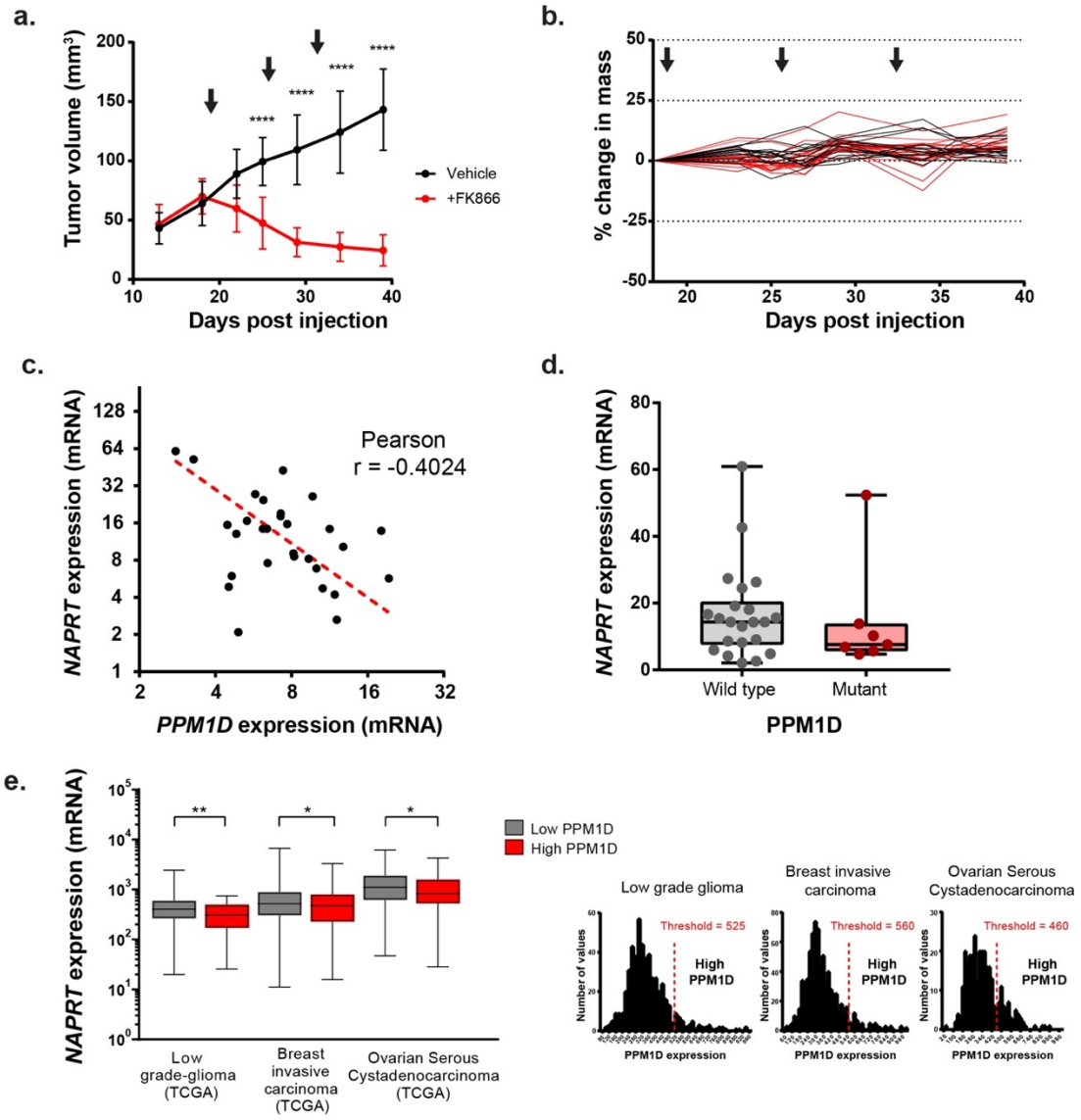

Supplementary Fig. 9. Applicability of NAMPT inhibitors for the treatment of *PPM1D* mutant, non-glioma tumors. (**a**) Tumor volume measurements of vehicle or FK866-treated athymic nude mice harboring U2OS cell line xenografts. FK866 treatment consisted of 20mg/kg BID for 3 four day weekly cycles, indicated by arrows (n=15 independent animals, **** $p<0.0001$ by Mann-Whitney U test). Error bars represent standard deviation of the mean. (**b**) Percent change in body mass, measured for each mouse during the duration of treatment described in a. (**c**) *NAPRT* and *PPM1D* expression levels from PNOC003 DIPG cohort (*32*) tumor samples. (**d**) Comparison of *NAPRT* expression levels in wild type and *PPM1D* mutant DIPG tumors from the cohort in c. (**e**) Comparison of *NAPRT* expression levels in *PPM1D* high and low expressing tumors, in cancer subtypes commonly found to have amplification of *PPM1D* (*left*); with histograms of *PPM1D* expression (*right*). * $p<0.05$ ** $p<0.01$ by Student's T test.

Supplementary Table 1. Synthetic lethal drug screen compounds and IC_{50} ratios.

Drug Name	Company (catalog)	Target	$IC_{50}\left(\frac{\text{Par. Astros.}}{\text{PPM1D}^{\text{trncs.}}}\right)$
FK866	Selleckchem (S2799)	NAMPT	9746.59
Aphidicolin	Tocris (5736)	Topoisomerase 2	1.75
TH287	Selleckchem (S7631)	MTH1	1.52
ETP 45658	Tocris (4702)	DNApk	1.51
TMZ	Selleckchem (S1237)	DNA damage	1.37
SP2509	Selleckchem (S7680)	LSD1	1.36
Olaparib	Selleckchem (S1060)	PARP	1.32
MMS	Sigma (129925)	DNA damage	1.28
RITA	Selleckchem (S2781)	p53	1.27
NU-7441	Selleckchem (S2638)	DNApk, others	1.26
KU-55933	Selleckchem (S1092)	ATM	1.18
Dexrazoxane	Selleckchem (S5651)	Blocks mitosis	1.17
TCS2312	Tocris (3038)	CHK1	1.13
Lomustine	Selleckchem (S1840)	DNA damage	1.10
MMC	Selleckchem (S8146)	DNA damage	1.08
Bendamustine	Selleckchem (S1212)	DNA damage	1.07
MLM324	Selleckchem (S7296)	JMJD2	1.02
BEZ-235	Selleckchem (S1009)	PI3K and mTOR	1.01
ATRN-19	Atrin Pharm.	ATR	1.01
Irinotecan	Selleckchem (S2217)	Topoisomerase 1	1.01
AZD6482	Selleckchem (S1462)	DNApk, others	1.00
Etoposide	Selleckchem (S1225)	Topoisomerase 2	1.00
GSK2879552	Selleckchem (S7796)	LSD1	1.00
BMN673	Selleckchem (S7048)	PARP	0.99
Topotecan	Selleckchem (S1231)	Topoisomerase 1	0.99
LSD1-C76	Xcessbio (M66045-2s)	LSD1	0.98
PIK 75	Selleckchem (S1205)	DNApk, others	0.97
NCS	Sigma (N9162)	DNA damage	0.94
VE822	Selleckchem (S7102)	ATR	0.93
MLN4924	Selleckchem (S7109)	NAE (NHEJ)	0.92
Cyclophosphamide	Selleckchem (S2057)	DNA damage	0.90
PD 407824	Tocris (2694)	CHK1/Wee1	0.83
TC-S 7010	Selleckchem (S1451)	Aurora A	0.78
AZD7762	Selleckchem (S1532)	CHK1/2	0.77
KU 0060648	Selleckchem (S8045)	DNApk, others	0.69
MK-1775	Selleckchem (S1525)	Wee1	0.63

Supplementary Table 2. Oligos and siRNA target sequences.

Name	Type	Sequence
PPM1D guide RNA top	gRNA oligo	ACACCGTTGAGGGTATGACTACACCTG
PPM1D guide RNA bottom	gRNA oligo	AAAACAGGTGTAGTCATACCCTCAACG
PPM1D gDNA sequencing (forward)	primer	GCATAGATTTGTTGAGTTCTGGG
PPM1D gDNA sequencing (reverse)	primer	AGCCCTCTTATATCCTAAGTTTGG
PPM1D site-directed mutagenesis	primer	CCAGTCAAGTCACTCGAGGAGGATCCATGA CCAAGGGTGAATTC
PPM1D site-directed mutagenesis	primer	GAATTCACCCTTGGTCATGGATCCTCCTCGA GTGACTTGACTGG
NAPRT promoter bisulfite sequencing (forward)	primer	CACCTCTGGTGACCAAGACC
NAPRT promoter bisulfite sequencing (reverse)	primer	GTGGCCTGGTAGAGGTCAGT
NAPRT qPCR (forward)	primer	CGAGAGGAGTTGGGTGACATCC
NAPRT qPCR (reverse)	primer	CCTATGGCGCACTCCCTGTG
NAPRT siRNA 9	target sequence	GCAACAACAUUGACGAGGA
NAPRT siRNA 10	target sequence	CUGGAAACAACACGAAUCA
NAPRT siRNA 11	target sequence	GGUAGAGCCCUGACUGGGA
NAPRT siRNA 12	target sequence	GGACAGUGGUGACCUGCUA